BILINGUAL PUBLISHING GROUP

Journal of Atmospheric Science Research

https://journals.bilpubgroup.com/index.php/jasr/index

ARTICLE

Assessment of the Intertropical Convergence Zone over the Atlantic Ocean through an Algorithm Based on Precipitation

Natan Chrysostomo de Oliveira Nogueira*, *Pedro Henrique Gomes Machado*, *Michelle Simões Reboita**, *André Luiz Reis

Natural Resources Institute, Federal University of Itajubá, Itajubá, Minas Gerais, 37500-903, Brazil

ABSTRACT

The Intertropical Convergence Zone (ITCZ) is a key atmospheric system on a global scale, primarily driven by trade wind convergence near the equator. The ITCZ plays a crucial role in modulating the climate of the borders of tropical continental areas. For instance, Northeastern Brazil experiences a climate influenced by the ITCZ over the Atlantic Ocean. In some periods, the ITCZ exhibits double bands, known as the double ITCZ. While the features of the ITCZ have been described using various approaches and atmospheric variables, there is still a lack of regional studies focusing on the ITCZ and double ITCZ in the Atlantic Ocean. In this context, the main goals of this study are (1) to describe a simple algorithm based on precipitation to identify the ITCZ and double ITCZ, (2) to present a climatology (1997–2022) of the position, width, and intensity of these two convective bands, and (3) to investigate variabilities in the ITCZ characteristics associated with anomalies of sea surface temperature (SST) in the tropical Pacific and Atlantic oceans. The double ITCZ typically occurs southward of the main cloud band, and between February and April, both bands are more distant (~4.5°). In the western sector of the Atlantic Ocean, the ITCZ and its double band extend to more southerly latitudes in austral autumn. Considering the entire Atlantic basin, the annual mean of the latitudinal position, width, and intensity of the ITCZ is 4.9°N, 4.2°, and 11 mm/day, respectively, while for the double ITCZ, it is 0.4°N, 2.6°, 10.3 mm/day, respectively. While the SST anomalies in the Pacific Ocean (El Niño and La Niña episodes) affect more the ITCZ width, the SST anomalies in the Tropical South Atlantic affect both its position and width.

Keywords: Double ITCZ; Precipitation; Latitudinal position; Northeastern Brazil; Atlantic Ocean; ENSO

*CORRESPONDING AUTHOR:
Michelle Simões Reboita, Natural Resources Institute, Federal University of Itajubá, Itajubá, Minas Gerais, 37500-903, Brazil;
Email: reboita@unifei.edu.br

ARTICLE INFO
Received: 30 December 2023 | Revised: 11 January 2024 | Accepted: 15 January 2024 | Published Online: 22 January 2024
DOI: https://doi.org/10.30564/jasr.v7i1.6188

CITATION
Nogueira, N.C.O., Machado, P.H.G., Reboita, M.S., et al., 2024. Assessment of the Intertropical Convergence Zone over the Atlantic Ocean through an Algorithm Based on Precipitation. Journal of Atmospheric Science Research. 7(1): 59–73. DOI: https://doi.org/10.30564/jasr.v7i1.6188

1. Introduction

The Intertropical Convergence Zone (ITCZ) is a large-scale atmospheric system originating from the ascending branch of the Hadley cell [1]. It manifests near the equator in various atmospheric fields as a band of trade wind convergence, minimum in atmospheric pressure, minimum in outgoing longwave radiation (OLR), deep convective clouds, and frequent intermittent rain events that transfer freshwater from the atmosphere to the ocean [2–11]. These characteristics do not necessarily occur simultaneously and/or in the same location [7,12]. The average annual position of the ITCZ globally is found slightly north of the equator due to the Atlantic Ocean's transport of energy northward across the equator, resulting in the Northern Hemisphere being warmer than the Southern Hemisphere [13]. However, throughout the seasons, the ITCZ exhibits spatial variability, migrating toward the summer hemisphere [1,3,14].

The cloudiness associated with the ITCZ plays a crucial role in the atmospheric energy balance by influencing albedo and releasing latent heat into the atmosphere [4,15]. Additionally, it significantly contributes to hydrological balances, accounting for 32% of global precipitation [16]. While the ITCZ is well-defined over oceans, its characterization over continental areas is more complex. Factors contributing to its complexity include the less homogenous nature of continental surfaces, and in some instances, the ITCZ is part of regional monsoons [12]. Therefore, considering continental areas, coastal regions are the most influenced by the ITCZ, as is the case with the coastline of Northeastern Brazil [17], which is influenced by the ITCZ over the Atlantic Ocean.

Globally the ITCZ has a wider extent in the Northern Hemisphere (200–600 km) than in the Southern Hemisphere (~ 300 km) [18,19]. Over the Atlantic Ocean, few studies are addressing the characteristics of the ITCZ. Some of them include: ITCZ is located farther north (~10°N), in September, and farther south (~4°S), between February and May [20–22]. Along the longitude of 27.5°W, the ITCZ exhibits maximum width (6°) between October and November and minimum width (3°) between January and March [22]. Observational longwave radiation data showed that the ITCZ is more intense in the central region of the Atlantic Ocean than near the coast of South America from July to December [23].

The ITCZ, over the Atlantic [24–26], Pacific [27–29] and Indian oceans [3], experiences episodes of double bands. In other words, there is a secondary band of the ITCZ that positions itself to the south of the main cloudy band. Over the Atlantic Ocean, in the climatology from 2010 to 2017 between December and April, these episodes are more frequent and last during the months of March and April [26]. Liu and Xie [25] suggest that the double ITCZ is caused by the deceleration of surface winds as they approach the cold upwelling water near the equator. Additionally, decreases in vertical mixing and increases in vertical wind shear in the atmospheric boundary layer may contribute to the deceleration of trade winds as they move from warmer to colder water. On the other hand, Talib et al. [31] mention that the controls of the location and intensity of the ITCZ remain a fundamental question in climate science. As the double ITCZ is associated with heavy rainfall and convection, its understanding is crucial for comprehending variations in rainfall distribution, particularly in proximity to continental areas.

The location and intensity of the ITCZ in the Atlantic Ocean can also be influenced by ocean-atmosphere interaction mechanisms such as the El Niño-Southern Oscillation (ENSO) phenomenon and sea surface temperature (SST) anomalies in the Tropical South Atlantic (TSA). Berry and Reeder [32] compared the global position of the ITCZ during El Niño (EN) and La Niña (LN) events. Over the Atlantic Ocean, the ITCZ is located southward during La Niña episodes compared to El Niño ones. A more regional study focusing on the north of Northeast Brazil by Xavier et al. [33] showed that during the rainy season in the region (February to May), the average position of the ITCZ in LN years is between 2°S and 4°S, which aligns with the climatological pattern. On the other hand, in EN years, the ITCZ migrates northward, approaching the equator. Therefore, the latitudinal migration of the ITCZ impacts rainfall in

the northern region of Northeast Brazil, so that very rainy years may be influenced by LN, and less rainy years by EN. However, Liu et al. [9] found little variability in the ITCZ in the Atlantic Ocean associated with different phases of the ENSO.

Some studies suggest that the variability of the ITCZ over the Atlantic Ocean, with its respective impact on the coast of Northeast Brazil, is more closely linked to SST anomalies in the TSA sector than with SST anomalies in the Pacific Ocean. More intense positive anomalies in the TSA than in the Tropical North Atlantic imply a southward migration of the ITCZ, contributing to rainfall on the coast of Northeast Brazil [34–36]. Other studies also emphasize that the combination of negative anomalies in the TSA concurrent with EN events affects the position of the ITCZ, leading to precipitation deficits in Northeast Brazil. On the other hand, positive anomalies occur when there are positive SST anomalies in the TSA and LN events occurring simultaneously [37].

Studies aiming to characterize the properties of the ITCZ such as its location, width, and intensity employ various approaches and atmospheric variables for system identification. For instance, Gadil and Guruprasad [38] utilized daily 2.5° data of OLR and albedo, applying thresholds: OLR < 185 W m^{-2} and albedo > 0.5. Grid points meeting these conditions were retained only if the conditions were satisfied by at least two of the eight neighboring grid points. Berry and Reeder [32] defined the ITCZ as the location where the magnitude of the horizontal gradient of divergence is zero, applying additional techniques to refine its location. Liu et al. [9] defined the ITCZ position based on the maximum zonal mean precipitation. The maximum zonal mean precipitation between 20°S–20°N is considered the ITCZ intensity, and the corresponding latitude is the ITCZ position. A similar methodology was used by Elsemüller [39], who quantified the latitudinal ITCZ mid-position based on the minimum convergence over longitudes. Samuel et al. [40] employed brightness temperature as a proxy for deep convective cloud cores, associating it with the ITCZ position. Carvalho and Oyama [22] characterized the properties of the ITCZ through pentad precipitation over a span of 10 years (1999 to 2008) with a data grid spacing of 1°. They used a threshold of approximately 7 mm/day to outline the region of ITCZ activity over the central Atlantic Ocean (27.5ºW).

Since the ITCZ over the Atlantic Ocean affects the weather and climate of the Northeastern region of Brazil, it is important to understand its main characteristics as well as the variability associated with some of the ocean-atmosphere interaction processes (teleconnection patterns). A more detailed description of the ITCZ over the Atlantic Ocean can also provide useful information for studies aimed at improving global and regional climate models. Hence, these are the motivations for this study.

Although there are studies about the ITCZ, most of them have a global perspective, which differs from the present study that focuses on a regional scale. Additionally, some methodologies for identifying the ITCZ are not very straightforward. Therefore, here we aim to develop a simple and efficient algorithm that can be adapted for any ocean basin (the same is available in a public database, see methodology) using one of the most widely observed variables globally, which is precipitation. Hence, the objectives of this study are (1) to describe the algorithm developed to record the position, width, and intensity of the ITCZ as well as its double band, (2) based on the application of the algorithm, to present the climatology of the basic characteristics of the ITCZ (position, width, and intensity) from 1997 to 2022, and (3) to investigate variabilities in the ITCZ characteristics associated with anomalies of SST in the tropical Pacific (EN and LN) and the Tropical South Atlantic.

2. Materials and methods

2.1 Study area

The study area comprises the region of the Tropical Atlantic Ocean situated between 10°S–18°N and 49°W–10°W, as defined previously [22] (blue box in **Figure 1**). **Figure 1** also shows two regions, Niño 3.4 (marked with a red box) and TSA (marked with

a green box), which are used to compute SST anomalies for analyzing their impact on ITCZ characteristics.

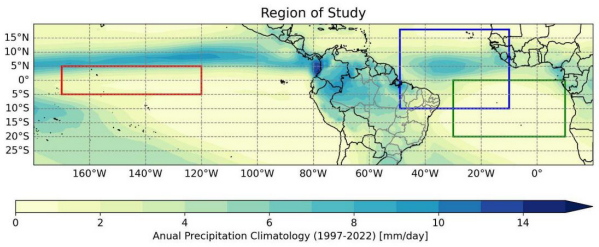

Figure 1. Study region (blue box), areas used to compute TSA (green box), and Niño 3.4 indices (red box). Global Precipitation Climatology Project (GPCP [41]) annual precipitation (mm/day) climatology from 1997 to 2022 is shown in shaded.

2.2 Data

Precipitation

Daily precipitation data from 1997 to 2022 used in this study were obtained from the Global Precipitation Climatology Project (GPCP) of the National Oceanic and Atmospheric Administration (NOAA) [41]. These data have a horizontal resolution of 1° × 1° and can be accessed at: https://www.ncei.noaa.gov/products/climate-data-records/precipitation-gpcp-daily.

Winds

Daily (0000 UTC) wind components (zonal, u, and meridional, v) at 10 meters above ground level were obtained from the ERA5 reanalysis [42]. ERA5 has a horizontal resolution of 0.25° × 0.25°, and data access is available through the Climate Data Store (CDS): https://cds.climate.copernicus.eu/cdsapp#!/dataset/reanalysis-era5-single-levels?tab=overview.

Climate indices

In this study, tree climate indices such as the Oceanic Niño Index (ONI) and TSA index. The different phases of ENSO were identified through the ONI, calculated monthly data from the NOAA within the Niño 3.4 region (**Figure 1**), and is available at: https://origin.cpc.ncep.noaa.gov/products/analysis_monitoring/ensostuff/ONI_v5.php. The TSA index, a monitoring index for the Tropical South Atlantic Ocean (**Figure 1**), was computed using NOAA Optimum Interpolation (OI) SST V2 (https://psl.noaa.gov/data/gridded/data.noaa.oisst.v2.html). This dataset has a horizontal resolution of 1° x 1°. The TSA index was obtained as follows: first, the monthly mean of SST and its anomaly is calculated in the box 30°W–10°E, 20°S–0° (**Figure 1**). Given the positive trend exhibited by this obtained time series, the trend is removed. This final result is the TSA index.

2.3 Methodology

Algorithm description for identifying the ITCZ

Although there are different ways to identify the ITCZ, we aimed for a simple methodology that would be easy to apply and use by other researchers interested in the subject. Thus, the algorithm described below is an adaptation of the methodology by Carvalho and Oyama [22], who identified the ITCZ in a single longitude band over the central Tropical Atlantic. Our algorithm is written in Python, uses only daily precipitation data converted into pentads, and is freely available on the GitHub platform: https://github.com/CATUnifei/ITCZ_code. The variable precipitation has one of the highest numbers of observations and estimates globally, and it is used in various studies for ITCZ identification [22,9].

General idea of the algorithm

1) The process begins by reading daily precipitation data in millimeters (mm) in NETCDF format and transforming the daily data into pentads (5-day averages). This allows the removal of high-frequency disturbances related to daily fluctuations [22].

2) The second step is to define the precipitation threshold that will be applied at each grid point to identify the ITCZ. Here, we defined the threshold as the average precipitation over the entire dataset period in the study area (**Figure 1**) plus one standard deviation (threshold = mean + one standard deviation). The values obtained were 3 mm/day for the average and 4 mm/day for the standard deviation, resulting in a threshold of 7 mm/day. It is a flexible threshold that the user can configure as a mean of a specific period, hence, being useful in climate change studies.

3) Grid points with precipitation greater than the

threshold (> 7 mm/day) are coded with the number 1 (true), otherwise, with 0 (false). This information is stored and will allow the identification of initial latitudes (Li) and final latitudes (Lf) (technical details are provided below).

4) Since the data are in grid points, a function is created to read their information at all latitudes. The data scan starts at the westernmost longitude and given latitudes from north to south; after scanning and identifying Li and Lf of the ITCZ band, the algorithm moves on to the next longitude. Two empty lists and three control variables are created, respectively, to store (a) Li and (b) Lf, and to have (c) a counter (cont), (d) a value accumulator (value), and (e) the ITCZ band number (n). This last information is because a double ITCZ band can also occur. To consider that there is an ITCZ band, it must have a minimum width of 2° latitude (2 grid points) where precipitation is above the threshold, meaning that for every two consecutive "1" in the column, the code records an ITCZ band.

This algorithm stands out by identifying both the primary and secondary bands of the ITCZ. Its steps are represented in **Figure 2**. Regarding the technical aspects of the code, a brief description is presented here.

Technical details of the algorithm

Initially, the variables cont, value, and n are set to zero; at the beginning of the process, 1 is added to cont, and the boolean (0 or 1) from the matrix is added to the value. After that, there are four situations:

1) If value = 1, Li is recorded, and the operation continues;

2) If value ≠ cont and value = 1, it indicates that there is no continuation of the ITCZ band because it lacks the prerequisite of 2 grid points, so cont and value are set to zero to proceed with the analysis;

3) If value ≠ cont and value = 0, it is verified that the ITCZ band, and cont and value are set to zero for the next analysis;

4) If value ≠ cont and value > 1, the previous latitude is recorded in Lf since the analysis stopped one latitude ahead, and "1" is added to n to indicate that the first ITCZ band has been found. Cont and value are reset to zero again in case the second ITCZ band can be found at the same longitude (column). The function then returns the values of Li and Lf to be stored in two arrays for the same ITCZ band number.

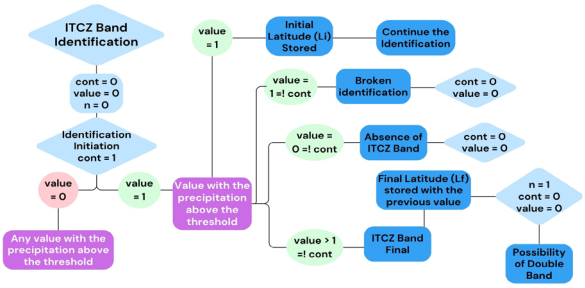

Figure 2. Flowchart of the algorithm steps for identifying the ITCZ bands.

As output, the algorithm provides, for each pentad and longitude, the initial latitude (Li) and final latitude (Lf) of the primary and secondary bands of the ITCZ, representing the position of the ITCZ. From this information, it is possible to obtain the width of each band in degrees (Lf-Li) and its mean position. The intensity of the ITCZ is calculated by averaging all grid points between Li and Lf for each longitude. Based on the algorithm output in pentads, monthly, seasonal, and annual climatologies can be calculated. In this study, the focus is the seasonal climatologies (position, width, and intensity of the ITCZ).

ITCZ variability

We also analyzed the characteristics of the ITCZ during EN and LN episodes and in different phases of the TSA index. The months with the occurrence of EN and LN events were selected in the time series of the ONI and separated by the season of the year. The ONI table provided by NOAA also includes the classification of the EN and LN periods. The next step was to calculate the average characteristics of the ITCZ during these seasonal periods with EN and LN occurrences and compare them with the climatology of the seasons. The same methodology was applied to analyze SST anomalies in the TSA region, except for the classification of the negative and positive phases of the TSA index. For this purpose, we first calculated the standard deviation of the time series. Then, we selected only the months with a TSA index

lower (higher) than one standard deviation for negative (positive index).

3. Results and discussion

3.1 Algorithm validation

Before applying the algorithm in any study, it is necessary to evaluate its performance. Validation was carried out by comparing the algorithm's results with the spatial map of precipitation, wind vectors at 10 meters height, and satellite images. One example is provided for the pentad from October 27 to October 31, 2022 (chosen aleatory) (**Figures 3 and 4**). As satellite images are not provided in pentads but at various times throughout the day, five images from the GOES-16 satellite in the visible channel were selected, one for each day of the pentad, and at 1200 UTC (**Figure 4**).

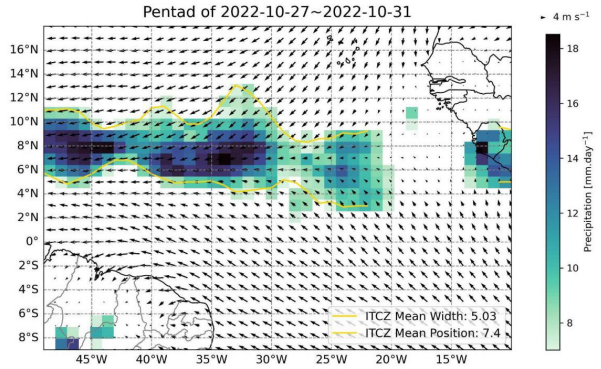

Figure 3. GPCP mean precipitation higher than 7 mm/day (shaded), wind intensity and direction at 10 m (m/s, black arrows), and the position of the ITCZ for the pentad from October 27th to October 31st, 2022. The initial (Li) and final (Lf) positions of the ITCZ are indicated by yellow lines. The mean position and width of the ITCZ are displayed at the bottom right of the panels.

In **Figure 3**, the band of precipitation > 7 mm/day is positioned approximately between 5° to 10°N and 50° to 20°W, which coincides with the region where the trade winds converge (arrows with larger size pointing south and meeting arrows with smaller size) and with the region of maximum cloudiness shown in the satellite images (**Figure 4**). The algorithm's result is represented by the two yellow lines delimiting the Li and Lf of the ITCZ (**Figure 3**). The algorithm captures the location of the rain well and does not show information between longitudes 20° to 13°W, where there is no precipitation and winds are weak (**Figure 3**). With Li and Lf, the width of the ITCZ can be estimated to be approximately 5° (500 km), consistent with satellite images and also with other studies [18,22].

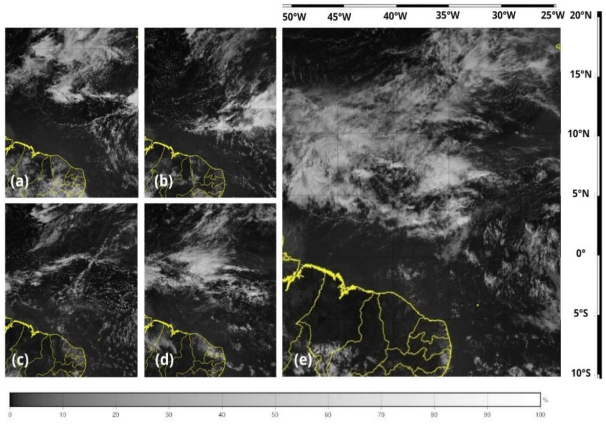

Figure 4. GOES-16 satellite image from visible channel 02 (0.64 microns) for October (a) 27, (b) 28, (c) 29, (d) 30, and (e) 31, 2022 at 1200 UTC.

Source: https://satelite.cptec.inpe.br

3.2 Seasonal climatology of the ITCZ

In this section, the seasonal climatology (**Figures 5 and 6**) of the position (Li, Lf and mean position), width, and intensity of the main band of the ITCZ (hereafter referred to as the ITCZ) and the secondary band (hereafter referred to as double ITCZ) are presented. **Figures 5 and 6** also show the spatial variability of these features.

In MAM, the ITCZ reaches its southernmost position in most of the Tropical Atlantic Ocean, with an average position of 1.4°N (**Figure 5b**). In this same season, in the western sector of the domain, the ITCZ is located between 2°N (Li) and 4°S (Lf), directly affecting the northern regions of North and Northeast Brazil. Meanwhile, in the center of the Tropical Atlantic (27.5°W), the mean position is around 1°N, consistent with Carvalho and Oyama [22]. The double ITCZ also occupies its southern position in MAM in the western sector of the domain (Li =

2°S, Lf = 5°S, and average = 3.5°S) (**Figure 5b**). The average width of the ITCZ and the double ITCZ is 4.14° and 2.44° (**Figures 6a and 6b**), respectively, and ITCZ is wider than in the other seasons west of 40°W. The intensity of the ITCZ and the double band is approximately 11.1 mm/day and 10.0 mm/day (average precipitation between Li and Lf, **Figures 6c and 6d**). Spatially, in MAM, precipitation shows higher volumes west of 30°W, near the North and Northeast regions of Brazil, which is in agreement with Kousky [23]. Additionally, these areas also exhibit higher standard deviation (**Figure 7b**).

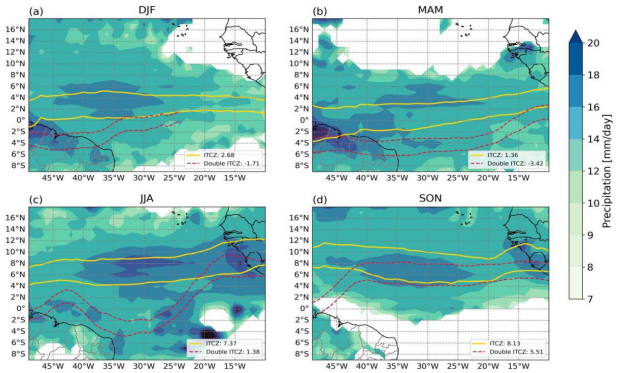

Figure 5. Seasonal climatology from 1997 to 2022 regarding the position of the ITCZ (yellow continuous lines) and double ITCZ (red dashed lines) for each longitude, as well as the spatial pattern of the precipitation > 7 mm/day (shaded): (a) DJF, (b) MAM, (c) JJA, (d) SON. The mean position of the ITCZ and the double ITCZ are displayed at the bottom right of the panels.

In JJA, the ITCZ migrates northward, positioning itself at an average of about 7.4° (**Figure 5c**). It is during this season that it reaches its northernmost position near the African continent (Li = 12°N and Lf = 6°N) and in the central Atlantic (Li = 9°N and Lf = 5°N), consistent with Carvalho et al. [22], who identified the northernmost position of the ITCZ to be approximately 8°N in August. The double ITCZ also migrates northward (average position of 1.4°N) but does not exhibit a zonal pattern like the ITCZ (**Figure 5c**). The average width of the ITCZ and the double ITCZ is approximately 4.4° and 2.6° (**Figures 6a and 6b**), respectively, while the average precipitation is 11.6 and 10.7 mm/day (**Figures 6c and 6d**). In JJA, the highest precipitation volumes and standard deviation occur in the central and eastern Atlantic within the latitude band of 4° to 8°N. Daily accumulations reach up to 13 mm/day (**Figures 5c and 6c**) with a standard deviation exceeding 6 mm/day (**Figure 7c**).

In SON, the ITCZ reaches its northernmost position in the western Atlantic (Li = 12°N and Lf = 8°N) and begins to migrate southward on the eastern side (Li = 10°N and Lf = 5°N). Its average position considering the entire Atlantic is 8°N (**Figure 5d**). In SON, the double ITCZ is also positioned further north (5.5°N). However, in the western sector of the Atlantic, the double ITCZ shows a southwestward tilt, affecting parts of the northern and northeastern regions of Brazil (**Figure 5d**). The average width of the ITCZ and the double ITCZ is approximately 4.6° and 3.2° (**Figures 6a and 6b**), respectively. At 27.5°W, the ITCZ has a width of 5° (~500 km), which is one degree smaller compared to Carvalho et al. [22]. This difference may be associated with the study period and different databases used in the works. The intensity of the ITCZ and the double ITCZ are 11.0 and 10.3 mm/day, respectively (**Figures 6c and 6d**). Analyzing the spatial distribution of precipitation, the highest accumulations and standard deviations are recorded between 40°W and 25°W and 4° and 8°N, with values of 11–12 mm/day (**Figures 5d**) and 6 mm/day, respectively (**Figure 7d**).

In DJF, the ITCZ and the double ITCZ begin to migrate southward, with average locations of 2.7°N and 1.7°S, respectively (**Figure 5a**). During this season, the double ITCZ is unable to configure itself to the east of 25°W (**Figure 5a**). The average width of the ITCZ and the double ITCZ is 3.5° and 2.2°, respectively (**Figures 6a and 6b**), while the intensity is 10.6 and 10.1 mm/day, respectively (**Figures 6c and 6d**). Additionally, in DJF, at 27.5°W, the width of the ITCZ of 3° aligns with the study [22]. Spatially, oceanic precipitation is maximum between 45° and 30°W and 0° and 7°N (**Figure 5a**), coinciding with the region of the highest standard deviation (> 6 mm/day, **Figure 7a**). Over the Brazilian coast, precipitation exhibits the highest volumes and standard deviation in MAM followed by DJF (**Figures 6 and**

7). This higher standard deviation may be associated with the variability of large-scale transient systems that affect the region, such as eastward wave disturbances, upper-level cyclonic vortices etc. [22,24,43–45].

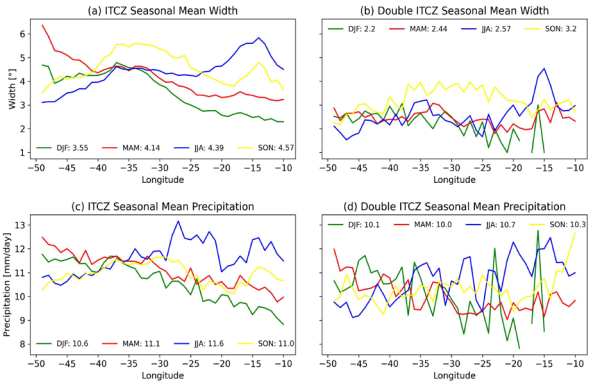

Figure 6. Seasonal climatology, from 1997 to 2022, of the width (degrees) of the (a) ITCZ and (b) double ITCZ for each longitude. The lines represent different seasons: DJF—green line, MAM—red line, JJA—blue line, and SON—yellow line). The mean width is also indicated in the panels.

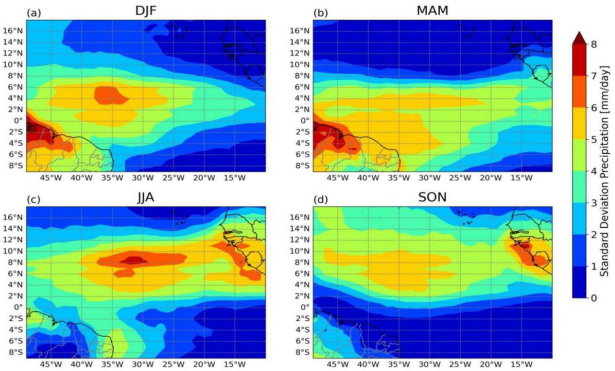

Figure 7. Seasonal standard deviation of the precipitation (mm/day) from 1997 to 2022: (a) DJF, (b) MAM, (c) JJA, (d) SON.

The seasonal frequency of the double ITCZ at various longitudes is depicted in **Figure 8**. Between 50°W and 42°W, the double ITCZ exhibits a similar higher frequency in both DJF and MAM, while to the east at 15°W, it is more frequent between JJA and SON. West of 30°W, on average, the double ITCZ occurs more frequently in MAM, agreeing with Teodoro et al. [26] (who focused on DJF and MAM only) and aligning with the practical knowledge of the third author in our study. When considering the entire Atlantic basin, events of the double ITCZ are slightly more prevalent in MAM (2 events) compared to other seasons.

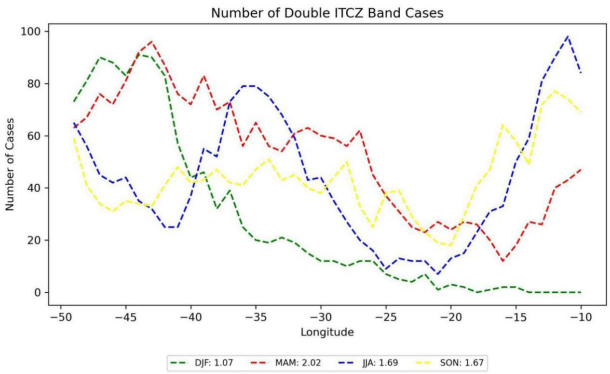

Figure 8. Seasonal frequency of the double ITCZ from 1997 to 2022 (DJF—green line, MAM—red line, JJA—blue line and SON—yellow line).

3.3 Monthly climatology of the ITCZ

To facilitate comparisons of the results with those from the literature, we also present monthly climatological values of the mean features (position, width, and intensity) for both the ITCZ and double ITCZ across the entire Tropical Atlantic basin (**Figure 9**). Additionally, **Figure 10** displays the monthly time series of the mean position for both the ITCZ and double ITCZ, aiming to identify any trends in these time series and emphasize the mean distance between the two bands.

Both the ITCZ and double ITCZ reach their northernmost position in September. The ITCZ shows Li at 12°N, Lf at 7.2°N, and a mean position of 9.6°N, while the double ITCZ has Li at 8.8°N, Lf at 5.5°N, and a mean position of 7.2°N (**Figure 9a**). Computing the difference between the mean positions of both bands, they are distant by 2.4°. When considering both Li and Lf, the southernmost position of the ITCZ occurs in March, with Li at around 2.1°N, Lf at approximately 1.6°S, and a mean position of about 0.24°N. However, when looking at only Lf, the most southern position occurs in both March and April. Applying the same criteria of Li and Lf, the double ITCZ has its southernmost position in February, with Li at approximately 3.3°S, Lf at around 5.2°S, and a mean position of 4.3°S (**Figure 9a**). But, considering only Lf, the most austral position occurs between February and April. During

this period of the year, both bands are distant by approximately 4.54°, aligning with the climatological value of 4° from December to May obtained by Teodoro et al. [26]. The annual cycle of the ITCZ position is consistent with some studies [20], which showed the ITCZ position in the west and east sectors of the Tropical Atlantic Ocean using various atmospheric variables.

The ITCZ has a greater width in August and September (~4.7°) and a smaller width in January (~3.4°), while the double ITCZ also exhibits a greater width in September (~3.3°) and a smaller width in February (~1.9°) (**Figure 9b**). The obtained values for the ITCZ are consistent with the global average for the Southern Hemisphere, which is approximately 3° (300 km) [18].

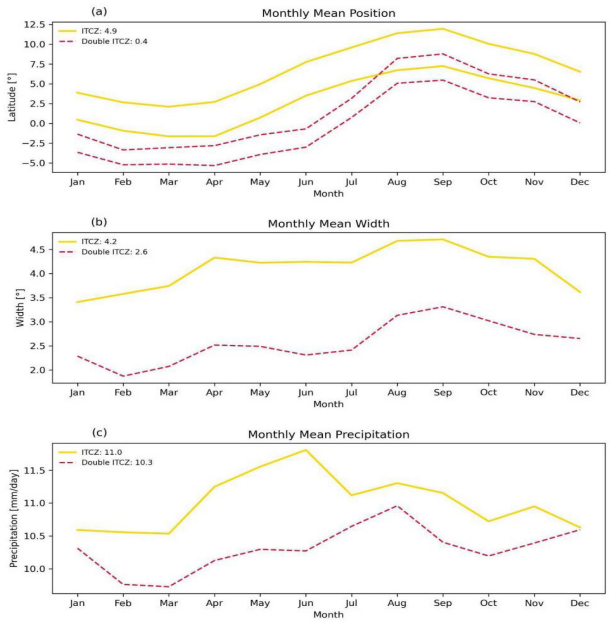

Figure 9. Annual cycle of the (a) position (degree latitude), (b) width (degree), and (c) intensity (mm/day) of ITCZ (yellow continuous lines) and double ITCZ (red dashed lines) from 1997 to 2022. Annual mean values are displayed in the upper left corner of the panels.

The ITCZ intensity is higher in June (~11.8 mm/day) and lower in March (~10.5 mm/day), while the double ITCZ exhibits its higher intensity in August (~11 mm/day) and lower intensity also in March (~9.7 mm/day) (**Figure 9c**). These results align with those for the central Tropical Atlantic obtained by Carvalho and Oyama [22]. According to these authors, the higher intensity of the ITCZ occurs between May and August (~13 mm/day), and the lower intensity between February and March (~10 mm/day). Xie et al. [6] also highlighted that in July-August, rainfall in the ITCZ is considerably stronger than in March-April, and this strengthening may be associated with the abundance of strong westward propagating easterly wave disturbances that help trigger convection over the ocean.

The time series of the monthly mean position of the ITCZ and double ITCZ exhibit a slightly southward trend, of –0.0036°/year and –0.02°/year, respectively, but without statistical significance (**Figure 10**). Liu et al. [9] depicted the annual time series of the ITCZ position in several locations globally. For the Atlantic Ocean (20°N–20°S and 49°W–9°W), **Figure 3d** also indicates a slightly negative trend between 1998 and 2018.

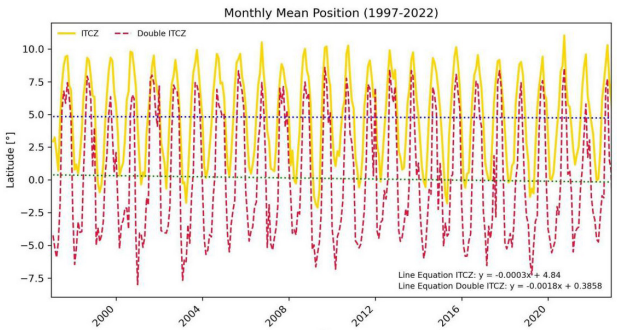

Figure 10. Monthly mean position (degree latitude) of the ITCZ (yellow continuous line) and double ITCZ (red dashed line) from 1997 to 2022. Linear trends are also depicted with dashed lines.

3.4 ITCZ interannual variability

ENSO

During the EN events, atmospheric convection intensifies in the central and eastern Tropical Pacific, leading to tropical tropospheric warming and anomalous subsidence over the tropical Atlantic, resulting in reduced precipitation [6]. On the other hand, during LN, it is expected that there will be more precipitation over the Tropical Atlantic. Indeed, **Figure 11** confirms the described pattern. In addition, it indicates that Northeast Brazil is more impacted by the ENSO phases in MAM (**Figures 11c and 11d**). To

verify if these spatial patterns of precipitation anomalies cause changes in the ITCZ position and width, **Figures 12 and 13** are presented.

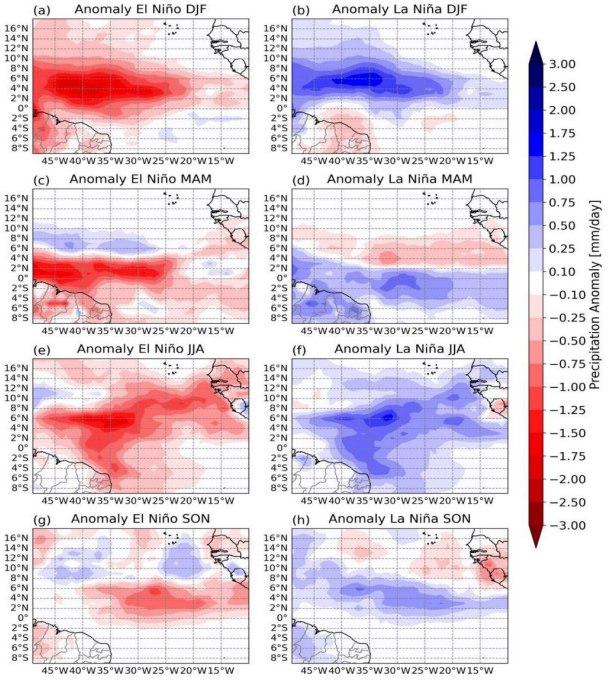

Figure 11. Seasonal precipitation anomaly (mm/day) in El Niño cases (left column) and La Niña cases (right column).

In periods with EN and LN, the mean position of the ITCZ is little affected, showing variations lower than 0.5° in comparison with the climatological value (**Figure 12**). On the other hand, when Li and Lf are individually analyzed, there are more variations, which affect the ITCZ width (**Figure 13**). During EN episodes in DJF, Li and Lf, west of 35°W, are displaced south compared to the climatological pattern (**Figure 12a**). In MAM, Lf, west of 35°W, is slightly retracted to the north (**Figure 12b**). In JJA and SON, Lf is also retracted to the north but over a larger extent in the central region of the oceanic basin (37.5°W to 17.5°W; **Figures 12c and 12d**). In SON, a difference is that Li, between 25°W and 17.5°W, is displaced to the north about climatology (**Figure 12d**). Considering LN episodes in DJF, west of 30°W, Li and Lf shift to the north about climatology (**Figure 12a**). In MAM, Lf moves south between 40°W and 20°W (**Figure 12b**). In the other seasons, Li and Lf have fewer differences about the climatological pattern. Our results partially support the findings [32], who emphasized that during the rainy season in the north of Northeast Brazil, the average position of the ITCZ in LN episodes aligns with the climatological pattern. However, they differ from those in EN episodes; during EN episodes, the ITCZ migrates northward, approaching the equator [32]. In our case, a higher change is observed in Lf rather than in both borders of the ITCZ.

In summary, during EN events, the ITCZ exhibits Lf slightly retracted to the north compared to the climatology. In LN events, both Li and Lf tend to be slightly more expanded than the climatology. These features impact the width of the ITCZ: during EN events, the ITCZ is narrower, whereas during LN events, the ITCZ is wider than in the climatology (**Figure 13**). The contraction of the ITCZ in EN events can reach up to 0.8° west of 35°W, except in SON. In JJA, the expansion of the ITCZ can reach 0.6° between 40°W and 30°W.

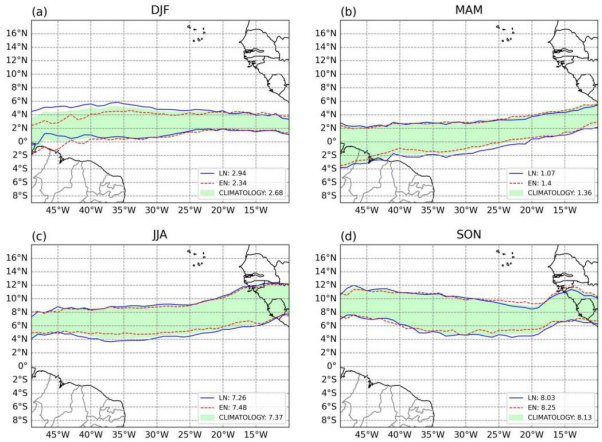

Figure 12. Climatological mean position (degrees) of the ITCZ (shaded), mean El Niño events (red dashed line), and during La Niña events (blue solid line). The mean position over the entire Atlantic is depicted in the bottom right of the panels.

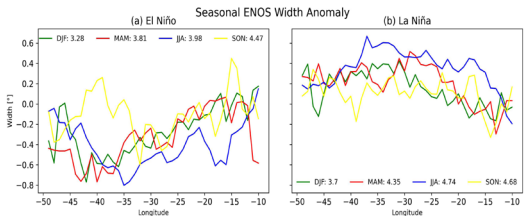

Figure 13. Seasonal anomaly of the mean width of the ITCZ in (a) El Niño (EN) and (b) La Niña (LN) events between 1997 and 2022. The mean width (degrees) of the ITCZ is also displayed in the panels.

TSA index

Figure 14 shows the spatial pattern of precipitation anomalies associated with different phases of the TSA index. Over the ocean, the ITCZ rainfall is intensified in its southern sector and weakened in its northern sector when a positive TSA index predominates (**Figures 14a, 14c, 14e, and 14g**). Conversely, precipitation anomalies of the opposite signal occur when a negative phase of the TSA index predominates (**Figures 14b, 14d, 14f, and 14h**). **Figure 14** also reveals that a great portion of the precipitation in the north and northeast sectors of Northeastern Brazil during MAM and JJA is influenced by SST anomalies in the TSA region.

A combined analysis of **Figures 11 and 14** corroborates the findings [36,37]. In other words, the negative (positive) phase of TSA and EN (LN) contribute to rainfall deficits (excess) in Northeastern Brazil.

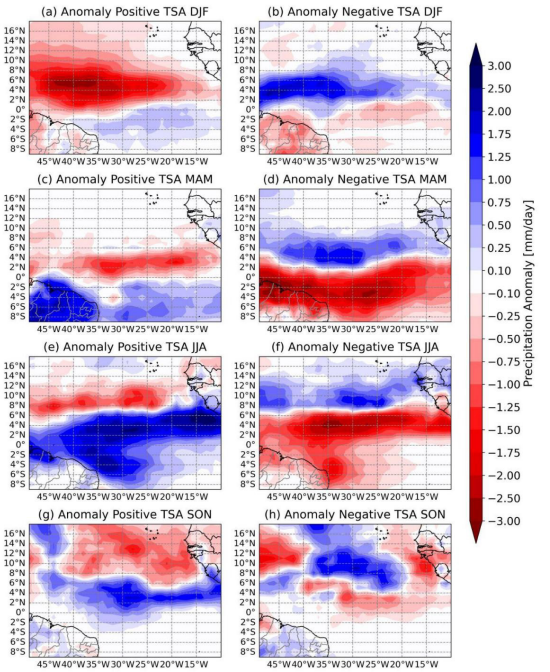

Figure 14. Seasonal precipitation anomaly (mm/day) in positive TSA index (left column) and negative TSA index (right column).

Figure 15 complements the results of **Figure 14** by showing the seasonal changes in the ITCZ position according to the dominant pattern of TSA anomalies. A positive TSA index is associated with the southward displacement of the ITCZ in all seasons. However, the mean position of the ITCZ is more southward displaced in DJF (0.97°), followed by JJA (0.72°), in relation to the climatology (**Figure 15**). The response of the ITCZ to a negative TSA index is a northward displacement, which, in terms of the mean position of the ITCZ, is higher in MAM (0.88°), followed by JJ (0.82°). SST anomalies also affect the width of the ITCZ. In the negative TSA index, generally, the ITCZ is narrower than the climatology except in SON between 40° and 30° W (**Figure 16b**). On the other hand, the width shows greater variability in the positive TSA index. The ITCZ is wider in JJA at all longitudes, and west of 40° W in MAM. Conversely, west of 25° W, the ITCZ is narrower than the climatology in DJF (**Figure 16a**).

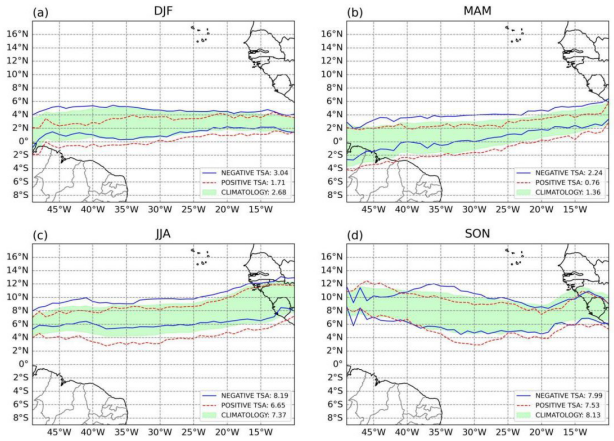

Figure 15. Climatological mean position (degrees) of the ITCZ (shaded), mean during positive TSA index (red dashed line), and negative TSA index (blue solid line). The mean position over the entire Atlantic is depicted in the bottom right of the panels.

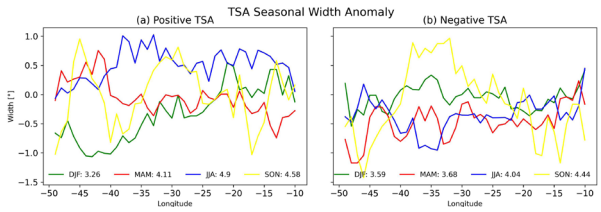

Figure 16. Seasonal anomaly of the mean width of the ITCZ in (a) positive TSA index and (b) negative TSA index between 1997 and 2022. The mean width (degrees) of the ITCZ is also displayed in the panels.

4. Conclusions

As the ITCZ is one of the large-scale precipitating systems that greatly influences the climate of

coastal tropical regions [17,46,47], the main objective of this study was to present an algorithm developed to locate both the primary and secondary bands (double ITCZ) of the ITCZ over the Atlantic basin. The algorithm identifies the initial (Li) and final (Lf) limits of the bands, providing information for the calculation of the average position, width, and intensity of the two bands. This algorithm is available on an open platform (https://github.com/CATUnifei/ITCZ_code) and can be easily adjusted for applications with other variables and in other oceanic basins. The study also aimed to present the climatology of the basic characteristics of the ITCZ and double ITCZ (position, width, and intensity) from 1997 to 2022 and to investigate variabilities in the ITCZ characteristics associated with anomalies of SST in the tropical Pacific (EN and LN) and the Tropical South Atlantic. The main findings are as follows:

Double ITCZ: It is located southward of the ITCZ with a mean distance reaching approximately 4.5° (computed considering the mean position of both bands) between February and April. West of 30°W, the double ITCZ occurs more frequently in MAM and has a mean position at 1°S, directly affecting the northern regions of North and Northeast Brazil. Considering the entire Tropical Atlantic Ocean, the double ITCZ shows a larger width (~3.3°) in September and a higher intensity (~11 mm/day) in August.

ITCZ: In MAM, the ITCZ reaches its southernmost position in most of the Tropical Atlantic Ocean, with an average position of 1.4°N. Considering the entire Tropical South Atlantic, the ITCZ shows a larger width (~4.7°) in August and September and a higher intensity (~11.8 mm/day) in June.

ITCZ interannual variability: Episodes of EN and LN affect the ITCZ width more, while SST anomalies in the TSA region affect both position and width. During EN and LN episodes, the mean position of the ITCZ is little affected, but changes in the limits of the ITCZ lead to alterations in width. Specifically, during EN events, the ITCZ is narrower, whereas during LN events, the ITCZ is generally wider than in the climatology. Considering the TSA index, a positive index is associated with the southward displacement of the ITCZ in all seasons, while a negative index indicates a northward displacement. Regarding the width, the ITCZ is generally narrower than the climatology during episodes of negative TSA index. On the other hand, the width exhibits greater variability during episodes of positive TSA index.

This study can serve as a guide for others, and we highlight that it is important to investigate the impact of other teleconnection mechanisms on the ITCZ and double ITCZ features.

Author Contributions

NCON: data collection, algorithm development, formal analysis and wrote the paper; PM: data collection, algorithm development, formal analysis and wrote the paper; MSR: conceived and designed the algorithm and analysis, wrote and reviewed the paper; ALR: algorithm development and reviewed the paper.

Conflict of Interest

The authors declare no conflict of interest.

Funding

This research was funded by Conselho Nacional de Pesquisas (CNPq), Fundação de Amparo à Pesquisa do Estado de Minas Gerais (FAPEMIG) and Coordenação de Aperfeiçoamento de Pessoal de Nível Superior (CAPES).

Acknowledgments

The authors thank all the meteorological centers that provided the datasets used in this study.

References

[1] Asnani, G.C., 1993. Tropical meteorology. Indian Institute of Tropical Meteorology: Pune.

[2] Waliser, D.E., Somerville, R.C.J., 1994. Preferred latitudes of the intertropical convergence zone. Journal of Atmospheric Sciences. 51(12),

1619–1639.
DOI: https://doi.org/10.1175/1520-0469(1994)051<1619:PLOTIC>2.0.CO;2

[3] Xie, S.P., Philander, S.G.H., 1994. A coupled ocean-atmosphere model of relevance to the ITCZ in the eastern Pacific. Tellus A. 46(4), 340–350.
DOI: https://doi.org/10.3402/tellusa.v46i4.15484

[4] Waliser, D.E., Gautier, C., 1993. A satellite-derived climatology of the ITCZ. Journal of Climate. 6(11), 2162–2174.
DOI: https://doi.org/10.1175/1520-0442(1993)006<2162:ASDCOT>2.0.CO;2

[5] Diaz, H.F., Bradley, R.S., 2004. The Hadley circulation: Present, past, and future. The Hadley circulation: Present, past and future. Advances in global change research. Springer: Dordrecht.
DOI: https://doi.org/10.1007/978-1-4020-2944-8_1

[6] Wang, C., Xie, S.P., Carton, J.A., 2004. Tropical Atlantic variability: Patterns, mechanisms, and impacts. Earth's Climate: The Ocean-Atmosphere Interaction. 147, 121–142.
DOI: https://doi.org/10.1029/147GM07

[7] Krishnamurti, T.N., Stefanova, L., Misra, V., 2013. Tropical meteorology—An introduction. Springer: New York.

[8] Aimola, L., Moura, M., 2016. The influence of the Atlantic Meridional overturning circulation in the definition of the mean position of the ITCZ north of the equator. A review. Revista Brasileira de Meteorologia. 31(4 suppl 1). (in Portuguese).
DOI: https://doi.org/10.1590/0102-778631231 4b20150059

[9] Liu, C., Liao, X., Qiu, J., et al., 2020. Observed variability of intertropical convergence zone over 1998–2018. Environmental Research Letters. 15(10), 104011.

[10] Iyer, S., Drushka, K., 2021. Turbulence within rain-formed fresh lenses during the SPURS-2 experiment. Journal of Physical Oceanography. 51(5), 1705–1721.
DOI: https://doi.org/10.1175/JPO-D-20-0303.1

[11] Windmiller, J.M., Stevens, B., 2023. The inner life of the Atlantic Intertropical Convergence Zone. Quarterly Journal of the Royal Meteorological Society.
DOI: https://doi.org/10.1002/qj.4610

[12] Misra, V., 2023. Intertropical Convergence Zone. An introduction to large-scale tropical meteorology. Springer: Cham. pp. 91–109.
DOI: https://doi.org/10.1007/978-3-031-12887-5_4

[13] Schneider, T., Bischoff, T., Haug, G., 2014. Migrations and dynamics of the intertropical convergence zone. Nature. 513, 45–53.
DOI: https://doi.org/10.1038/nature13636

[14] Philander, S.G.H., Gu, D., Lambert, G., et al., 1996. Why the ITCZ is mostly north of the equator. Journal of Climate. 9(12), 2958–2972.
DOI: https://doi.org/10.1175/1520-0442(1996)009<2958:WTIIMN>2.0.CO;2

[15] Bony, S., Stevens, B., Frierson, D.M.W., et al., 2015. Clouds, circulation and climate sensitivity. Nature Geoscience. 8, 261–268.
DOI: https://doi.org/10.1038/ngeo2398

[16] Kang, S.M., Shin, Y., Xie, S.P., 2018. Extratropical forcing and tropical rainfall distribution: Energetics framework and ocean Ekman advection. npj Climate and Atmospheric Science. 1, 20172.
DOI: https://doi.org/10.1038/s41612-017-0004-6

[17] Tomaziello, A.C.N., Carvalho, L.M.V., Gandu, A.W., 2016. Intraseasonal variability of the Atlantic Intertropical Convergence Zone during austral summer and winter. Climate Dynamics. 47, 1717–1733.
DOI: https://doi.org/10.1007/s00382-015-2929-y

[18] Khrgian, A., 1977. Physical meteorology. Summaries of scientific progress: Meteorology and climatology, Volume 2. G.K. Hall: Boston.

[19] Monsoons [Internet]. World Meteorological Organization (WMO); 1986. Available from: https://library.wmo.int/idurl/4/37019

[20] Hastenrath, S., 1991. Climate dynamics of the tropics. Kluwer Academic Publishers: Dordrecht.

[21] Mendonça, F., Danni-Oliveira, I.M., 2007. Climatology: Basic concepts and Brazilian climatates. Oficina de Textos Publisher: São Paulo. (in Portuguese).

[22] Carvalho, M.A.V., Oyama, M.D., 2013. Atlantic Intertropical Convergence Zone width and intensity variability: Observational aspects. Revista Brasileira de Meteorologia. 28(3), 305–316. (in Portuguese).
DOI: https://doi.org/10.1590/S0102-77862013000300007

[23] Kousky, V.E., 1988. Pentad outgoing longwave radiation climatology for the South American sector. Revista Brasileira de Meteorologia. 3(1), 217–231.

[24] Uvo, C. R. B., 1989. The Intertropical Convergence Zone (ITCZ) and its relationship with precipitation in the northern region of northeast Brazil. (in Portuguese).

[25] Liu, W.T., Xie, X., 2002. Double intertropical convergence zones—A new look using scatterometer. Geophysical Research Letters. 29(22), 291–294.
DOI: https://doi.org/10.1029/2002GL015431

[26] Teodoro, T.A., Reboita, M.S., Escobar, G.C.J., 2019. Characterization of the double band of the Intertropical Convergence Zone (ITCZ) over the Atlantic Ocean. Yearbook of the Institute of Geosciences. 42(2), 282–298. (in Portuguese).
DOI: https://doi.org/10.11137/2019_2_282_298

[27] Hubert, L.F., Krueger, A.F., Winston, J.S., 1969. The double intertropical convergence zone-fact or fiction? Journal of the Atmospheric Sciences. 26(4), 771–773.
DOI: https://doi.org/10.1175/1520-0469(1969)026<0771:TDICZF>2.0.CO;2

[28] Zhang, C., 2001. Double ITCZs. Journal of Geophysical Research: Atmospheres. 106(D11), 11785–11792.
DOI: https://doi.org/10.1029/2001JD900046

[29] Henke, D., Smyth, P., Haffke, C., et al., 2012. Automated analysis of the temporal behavior of the double Intertropical Convergence Zone over the east Pacific. Remote Sensing of Environment. 123, 418–433.
DOI: https://doi.org/10.1016/j.rse.2012.03.022

[30] Meenu, S., Rajeev, K., Parameswaran, K., et al., 2007. Characteristics of the double intertropical convergence zone over the tropical Indian Ocean. Journal of Geophysical Research: Atmospheres. 112(D11).
DOI: https://doi.org/10.1029/2006JD007950

[31] Talib, J., Woolnough, S.J., Klingaman, N.P., et al., 2018. The role of the cloud radiative effect in the sensitivity of the intertropical convergence zone to convective mixing. Journal of Climate. 31(17), 6821–6838.
DOI: https://doi.org/10.1175/JCLI-D-17-0794.1

[32] Berry, G., Reeder, M.J., 2014. Objective identification of the intertropical convergence zone: Climatology and trends from the ERA-Interim. Journal of Climate. 27(5), 1894–1909.
DOI: https://doi.org/10.1175/JCLI-D-13-00339.1

[33] Teresinha de Maria Bezerra, X., Tércio, A., Maria Elisa S, S., 2017. Applications of models and techniques in the detection of climate variability and extremes. Bank of Northeast Brazil. (in Portuguese).

[34] Hastenrath, S., Greischar, L., 1993. Circulation mechanisms related to northeast Brazil rainfall anomalies. Journal of Geophysical Research: Atmospheres. 98(D3), 5093–5102.
DOI: https://doi.org/10.1029/92JD02646

[35] Reboita, M.S., Santos, I.A., 2014. Teleconnection influences in some precipitation standards. Brazilian Journal of Climatology. 15, 28–48. (in Portuguese).
DOI: https://doi.org/10.5380/abclima.v15i0.37686

[36] Reboita, M.S., Ambrizzi, T., Crespo, N.M., et al., 2021. Impacts of teleconnection patterns on South America climate. Annals of the New

York Academy of Sciences. 1504(1), 116–153. DOI: https://doi.org/10.1111/nyas.14592

[37] Pezzi, L., Cavalcanti, I., 2001. The relative importance of ENSO and tropical Atlantic sea surface temperature anomalies for seasonal precipitation over South America: A numerical study. Climate Dynamics. 17, 205–212. DOI: https://doi.org/10.1007/s003820000104

[38] Gadgil, S., Guruprasad, A., 1990. An objective method for the identification of the intertropical convergence zone. Journal of Climate. 3(5), 558–567. DOI: https://doi.org/10.1175/1520-0442(1990)003<0558:AOMFTI>2.0.CO;2

[39] Elsemüller, L., 2021. Quantifying the Intertropical Convergence Zone using wind convergences [Master's thesis]. Tübingen: Eberhard Karls Universität Tübingen.

[40] Samuel, S., Mathew, N., Sathiyamoorthy, V., 2023. Characterization of intertropical convergence zone using SAPHIR/Megha-Tropiques satellite brightness temperature data. Climate Dynamics. 60, 3765–3783. DOI: https://doi.org/10.1007/s00382-022-06549-x

[41] Adler, R.F., Gu, G., Sapiano, M., et al., 2017. Global precipitation: Means, variations and trends during the satellite era (1979–2014). Surveys in Geophysics. 38, 679–699. DOI: https://doi.org/10.1007/s10712-017-9416-4

[42] Hersbach, H., Bell, B., Berrisford, P., et al., 2020. The ERA5 global reanalysis. Quarterly Journal of the Royal Meteorological Society. 146(730), 1999–2049. DOI: https://doi.org/10.1002/qj.3803

[43] Study of the vertical and horizontal structure of precipitation and atmospheric circulation in the region of the ITCZ, 2002. (in Portuguese).

[44] Gomes, H.B., Ambrizzi, T., Pontes da Silva, B.F., et al., 2019. Climatology of easterly wave disturbances over the tropical South Atlantic. Climate Dynamics. 53, 1393–1411. DOI: https://doi.org/10.1007/s00382-019-04667-7

[45] Ferreira, G.W.S., Reboita, M.S., da Rocha, R.P., 2020. Upper level cyclonic vortices in the vicinity of Northeast Brazil: Climatology and analysis of the isentropic potential vorticity. Yearbook of the Institute of Geosciences. 42(3), 568–585. (in Portuguese). DOI: https://doi.org/10.11137/2019_3_568_585

[46] Jafari, M., Lashkari, H., 2020. Study of the relationship between the intertropical convergence zone expansion and the precipitation in the southern half of Iran. Journal of Atmospheric and Solar-Terrestrial Physics. 210, 105439. DOI: https://doi.org/10.1016/j.jastp.2020.105439

[47] Lashkari, H., Jafari, M., 2021. Annual displacement and appropriate index to determine ITCZ position in East Africa and the Indian Ocean regions. Meteorology and Atmospheric Physics. 133, 1111–1126. DOI: https://doi.org/10.1007/s00703-021-00797-y